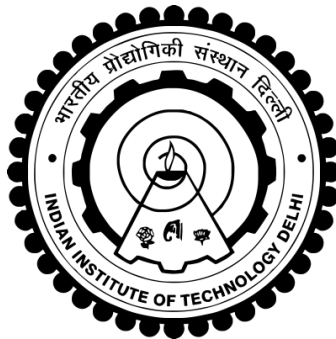


**FRACTURE BEHAVIOR OF ALUMINUM/ALUMINA AND
ALUMINUM/BORON CARBIDE FUNCTIONALLY GRADED
MATERIALS**

VINOD KUMAR PANDEY



**DEPARTMENT OF APPLIED MECHANICS
INDIAN INSTITUTE OF TECHNOLOGY DELHI
AUGUST 2019**

© Indian Institute of Technology Delhi (IITD), New Delhi, 2019

**FRACTURE BEHAVIOR OF ALUMINUM/ALUMINA AND
ALUMINUM/BORON CARBIDE FUNCTIONALLY GRADED
MATERIALS**

by

VINOD KUMAR PANDEY

Department of Applied Mechanics

Submitted

in fulfilment of the requirements of the degree of Doctor of Philosophy

to the



INDIAN INSTITUTE OF TECHNOLOGY DELHI

AUGUST 2019

Dedicated to

My beautiful wife, Sunanda and ever curious son- Sakshim & daughter Sandali

Without them my world would not be nearly as colorful

Certificate

This is to certify that the thesis entitled “**Fracture Behavior of Aluminum/Alumina and Aluminum/Boron Carbide Functionally Graded Materials**” being submitted by **Mr. Vinod Kumar Pandey** to the Indian Institute of Technology Delhi for the award of degree of **Doctor of Philosophy** in Applied Mechanics is a record of original, bonafide research work carried out by him under our supervision and guidance. The thesis work, in our opinion, has reached the requisite standard fulfilling the requirements for the degree of Doctor of Philosophy.

The results contained in this thesis have not been submitted in part or in full, to any other university or institute for the award of any degree or diploma.

(S Guruprasad)

Distinguish Scientist

DRDO HQR,

DRDO Bhawan

New Delhi, 110016, India

(B. P. Patel)

Professor

Department of Applied Mechanics

Indian Institute of Technology Delhi

New Delhi, 110016, India

Date: August, 2019

Place: New Delhi

Acknowledgements

I would like to express my deep sense of gratitude and appreciation to my esteemed supervisors Prof. B. P. Patel and Dr. S Guruprasad for their expert guidance, encouragement and invaluable help at every stage of my research. These words are inadequate to express the great care and interest taken by them in all aspects of the present work, without which this work would be a dream for me.

I wish to express my sincere thanks to my research committee members for their reviews, discussions and comments on the work. I would also like to express special thanks and gratitude to all the faculty and staff members of Department of Applied Mechanics, Indian Institute of Technology Delhi, New Delhi, for their kind help and support. I would like to extend very special thanks to Shri VV Parlikar (Director, R&DE (E)), my senior colleague Shri N B Vijayakumar, Shri A K Patel, Shri AK Sivanandan, Shri Naresh Kumar and Shri G K Sarkar for motivation, cooperation and support during this work. I also thank my office friends specially Shri A K Singh, Shri Aritra Hazra, Shri Jagmindar, Shri Abdul Kadir, Shri Sunil, Shri Sarang, Shri Dheerendra Yadav, Ravikant and other colleagues.

I would like to give special thanks to Prof. Uma Batra (Director, Punjab Engineering College, Chandigarh), Prof. N. B. Dhokey (HOD, Department of metallurgy and Materials Science, College of Engineering, Pune) for providing metallurgical/materials characterization supports, Mr. G.S. Kalgutkar (Owner Supercut Tools Co, Mumbai) for providing his resources in samples preparation, Mr. Anil Kumar (Lab Assistant (MTS), IIT Delhi), Shri Vinod Murkute (Technical Officer, R&DE(E), Pune), Mr. Rishi (Lab Assistant, IIT Delhi) for providing testing supports, Dr. Ruchita Pal (In Charge microscopy, JNU, New Delhi), Mr. Mohinder Singh (In Charge SEM, Punjab University,

Chandigarh) for help in sample characterization using SEM. I thank my childhood friends (Guddu and Raju) and research scholars of the department for their wonderful company and for making my association a very enjoyable and enriching experience at Indian Institute of Technology Delhi, New Delhi.

At last but certainly not the least, I would like to express my gratitude to parents, father-in-law, mother-in-law and my family members especially my eldest brother Shri Arun Pandey, my wife-Sunanda, Son-Saksham and daughter-Sandali for their endless love, continuous encouragement, moral support and cooperation by taking pain by controlling house in my absence during execution of my Ph.D work. This accomplishment would not have been possible without them. Thank you all.

(Vinod Kumar Pandey)

Abstract

Aluminum is used in aerospace and automotive industries owing to its low density, high thermal conductivity, high specific strength, stiffness and better ductility. Aluminum alloys have limitation of low hardness and poor wear resistance leading to restricted high performance applications. Aluminum based metal matrix composites (AMMCs) with ceramic (alumina and boron carbide) as reinforcement agents are gaining popularity. Further, gradation in properties is effective method to improve fracture properties and structural integrity of aluminum based metal matrix composites.

In the available literatures, 0.2% yield stress, ultimate tensile strength and elongation of Al/Al₂O₃ are addressed up to 30% of alumina whereas elastic properties of Al/Al₂O₃ and Al/B₄C composites are covered only up to 10% weight fraction of ceramic without even comparative studies of experimental and predicted elastic properties. To the best of the author's knowledge, fracture toughness, its variation with ceramic particle size and the experimental quasi static crack growth studies of functionally graded materials using crack gauge including Al/Al₂O₃ FGM have not been reported.

This thesis deals with various characterisations (metallurgical, mechanical, fracture and quasi static crack growth) of Al/Al₂O₃ (up to 50% weight fraction of alumina) and Al/B₄C (up to 35% weight fraction of boron carbide) composites (non-FGM) and FGMs. The samples are prepared using hot isostatic sintering at optimised parameters of 600°C, 30 MPa for 90 minutes having porosity less than 2% with uniform microstructure (measured through optical microscope and SEM) except for weight fractions of Al₂O₃ greater than 40% and B₄C greater than 30% without any other phase formation (confirmed through XRD and EDS).

The experimental Young's modulus is compared with micromechanics prediction techniques and is found to lie closely between Ravichandran's/Hashin-Shtrikman lower and Ravichandran's upper bounds for Al/Al₂O₃ and Al/B₄C composites, and close to self-consistent/Miller-Lannutti methods based single value predictions for Al/Al₂O₃ and modified rule of mixture, fuzzy logic and self-consistent methods predictions for Al/B₄C. The experimental Poisson's ratio, Charpy energy measured through non-FGM samples and hardness through FGM and non-FGM samples are compared with micromechanics prediction techniques. 0.2% yield stress, ultimate tensile strength (UTS) and Young's modulus increase whereas the fracture strain/ductility reduce with increase in weight fraction of Al₂O₃ up to 40%. Ductile fracture with reducing dimple size up to 30% weight fraction of Al₂O₃ and cleavage fracture for Al₂O₃ greater than 30% are observed for Al/Al₂O₃ composites.

Fracture toughness reduces with increase in weight fraction of ceramic and lies closely between Raveendran's lower and upper bounds, and close to Raveendran effective value for Al/Al₂O₃ and Al/B₄C composites.

Quasi static crack growth study indicates that crack on stiff side undergoes stable crack growth with mixed mode failure with deviation from straight path, whereas crack on compliance side undergoes unstable crack growth with crack moving in straight line path with mode-I failure.

सारांश

कम घनत्व, उच्च ऊष्मा चालकता, उच्च विशिष्ट सामर्थ्य, उच्च विशिष्ट यंग मापांक और बेहतर लचीलेपन के कारण अंतरिक्षयांत्रिकी और मोटरयांत्रिकी उद्योगों में एल्यूमीनियम का उपयोग किया जाता है। एल्युमिनियम मिश्र धातु की कम कठोरता और कम घर्षण प्रतिरोध के कारण इसका उपयोग उच्च प्रदर्शन अनुप्रयोगों में सीमित है। सुदृढीकरण एजेंटों के रूप में सिरामिक (एल्यूमिना और बोरान कार्बाइड) के साथ एल्यूमीनियम आधारित धातु मैट्रिक्स कंपोजिट (एएमएमसी) उपयोगी सिद्ध हुये हैं। इसके अलावा, फ्रैक्चर गुणों और एल्यूमीनियम आधारित धातु मैट्रिक्स कंपोजिट की संरचनात्मक अखंडता में सुधार करने के लिए गुणों में प्रवणता प्रभावी तरीका है।

उपलब्ध साहित्य में, एल्यूमीनियम/एल्यूमिना और एल्यूमीनियम/बोरान कार्बाइड के 0.2% प्रूफ प्रतिबल, अधिकतम तनाव सामर्थ्य और तन्यता को एल्यूमिना के 30% तक अध्ययन किया गया है, जबकि एल्यूमीनियम/एल्यूमिना कंपोजिट के प्रत्यास्थता गुणों का अध्ययन सिरामिक के केवल 10% वजन अंश तक किया गया है। प्रायोगिक और अनुमानित प्रत्यास्थता गुणों का तुलनात्मक अध्ययन भी उपलब्ध साहित्य में नहीं किया गया है। लेखक की जानकारी के अनुसार, एल्यूमीनियम/एल्यूमिना सहित एफजीएम की टफनेस, सिरामिक कण आकार के साथ इसकी प्रवणता और अर्ध स्थैतिक दरार वृद्धि का विश्लेषण दरार गेज का उपयोग करते हुए अध्ययन नहीं किये गए हैं।

यह शोधग्रन्थ, Al/Al₂O₃ (अल्युमिना के 50% वजन अंश तक) और Al/B₄C (बोरान कार्बाइड के 35% वजन अंश तक) कंपोजिट (गैर एफजीएम और एफजीएम) के विभिन्न लक्षणों (धातु विज्ञानीय, यांत्रिक, टफनेस और अर्धस्थैतिक दरार वृद्धि) से संबंधित है। प्रत्यास्थता एवं सामर्थ्य गुणों के अध्ययन के लिए नमूने गर्म आइसोस्टैटिक सिंटरिंग (उपयुक्त सिंटरिंग तापमान = 600°C, दाब=30 MPa, अवधि=90 मिनट) का उपयोग करके तैयार किये गए हैं। तैयार किये गए नमूने, Al₂O₃ के 40% तथा B₄C के 30% वजन अंशों तक एक सामान सूक्ष्म संरचना (प्रकाशीय सूक्ष्मदर्शी और ऐसइएम के द्वारा अध्ययन), 2% से कम सरंधता वाले तथा बिना अन्य फेज की उत्पत्ति (एक्सआरडी तथा इडीएस से पुस्टीकरण) वाले पाए गए हैं।

प्रयोगात्मक यंग मापांक की तुलना माइक्रोमैकेनिक्स अनुमानों से की गयी है। इस अध्ययन से, Al/Al₂O₃ तथा Al/B₄C के प्रयोगात्मक यंग मापांक रविचन्द्रन/हशीन-

स्ट्रीकमैन के न्यूनतम तथा रविचन्द्रन के अधिकतम मापो के बीच पाए गए हैं। Al/Al_2O_3 के प्रयोगात्मक यंग मापांक, सेल्फ कंसिस्टेंट/मिलर-लानुटी तथा माडीफाइड रूल ऑफ़ मिक्चर, फजी लॉजिक और सेल्फ कंसिस्टेंट अनुमानों के क्रमशः नजदीक पाये गये हैं। प्रयोगात्मक पोइसन अनुपात, चारपी ऊर्जा (गैर एफजीएम द्वारा मापे गये) तथा एफजीएम और गैर एफजीएम द्वारा मापी गयी कठोरता की तुलना माइक्रो मैकेनिक्स अनुमानों से की गयी हैं।

Al_2O_3 के 40% वजन अंश तक 0.2% प्रूफ सामर्थ्य, अधिकतम तनाव सामर्थ्य (यूटीएस) और यंग मापांक में वृद्धि दर्शायी गयी हैं, जबकि फ्रैक्चर विकृति/लचीलापन Al_2O_3 के वजन अंश में 40% तक की वृद्धि के साथ कम होते हैं। Al_2O_3 के 30% वजन अंश तक, डिम्पल के आकार में कमी के साथ डकटाइल फ्रैक्चर तथा Al_2O_3 के 30% से अधिक वजन अंश के लिए, क्लीवेज फ्रैक्चर का अवलोकन Al/Al_2O_3 कम्पोजिट के लिए किया गया है।

एल्यूमीनियम/एल्यूमिना और एल्यूमीनियम/बोरान कार्बाइड कंपोजिट की फ्रैक्चर टफनेस, सिरामिक के वजन अंश में वृद्धि के साथ कम होती पायी गयी है। यह रवींद्रन के निचले और ऊपरी सीमा के बीच, तथा रवींद्रन प्रभावी मूल्य के करीब पायी गयी है। अर्धस्थैतिक दरार का अध्ययन यह बताता है कि अधिक यंग मापांक की तरफ स्थित दरार की वृद्धि स्थिर और मिक्स्ड मोड फेलयोर के साथ सीधे पथ से विचलित पायी गयी है। जबकि कम यंग मापांक की तरफ स्थित दरार की वृद्धि अस्थिर और मोड-I फेलयोर के साथ सीधे पथ पर होती हुई पायी गयी हैं।

Table of Contents

Certificate		<i>i</i>
Acknowledgements		<i>ii</i>
Abstract		<i>iv</i>
Table of Contents		<i>viii</i>
List of Figures		<i>xiii</i>
List of Tables		<i>xviii</i>
Nomenclature		<i>xx</i>
Abbreviation		<i>xxv</i>
Chapter 1	Introduction and Literature Review	1
1.1	Introduction	1
1.2	Literature review	6
1.2.1	Fabrication techniques of functionally graded materials (FGM)	6
1.2.1.1	Vapor deposition technique	6
1.2.1.2	Powder metallurgy	7
1.2.1.3	Centrifugal casting	8
1.2.1.4	Solid freeform fabrication method	9
1.2.2	Mechanical characteriasation of FGM/non-FGM	9
1.2.2.1	Elastic constants	9
1.2.2.2	Strength and hardness	12
1.2.3	Crack tip stresses in FGMs	13
1.2.3.1	Stress singularity	13

1.2.3.2	Stress field asymmetry	17
1.2.4	Fracture characterisation of FGM/non-FGM	18
1.2.5	Crack growth of FGM	19
1.2.6	Crack perpendicular to material gradation direction	20
1.2.7	Crack parallel to gradation direction	22
1.2.8	Mixed mode	24
1.2.9	J-Integral	25
1.3	Micromechanics prediction techniques	26
1.3.1	Bound based techniques for elastic constants	26
1.3.1.1	Hashin- Shtrikman (H-S) bounds	26
1.3.1.2	Ravichandran's bound	27
1.3.1.3	Modified unit cell model	27
1.3.2	Single value based techniques for elastic constants	28
1.3.2.1	Modified rule of mixture (MROM)	28
1.3.2.2	Self consistent method (SCM)	29
1.3.2.3	Mori-Tanaka method (MTM)	30
1.3.2.4	Wakashima and Tsukamoto method (WTM)	30
1.3.2.5	Kerner method (KM)	30
1.3.2.6	Fuzzy logic method (FLM)	31
1.3.2.7	Miller and Lannutti method (MLM)	31
1.3.2.8	Hopkins-Chamis method (HCM)	32
1.3.2.9	Coherent Potential approximation (CPA)	32
1.3.3	Micromechanics prediction techniques for fracture toughness	32
1.4	Motivation and objectives	33

1.5	Novelty	37
1.6	Organization of the thesis	39
Chapter 2	Fabrication of non functionally graded and functionally graded materials specimens	40
2.1	Introduction	40
2.2	Powder characterisation	40
2.2.1	Wavelength dispersive X-ray fluorescence (XRF)	40
2.2.2	X-ray diffraction (XRD)	43
2.2.3	Scanning electron microscopy (SEM)	45
2.3	Design of samples	49
2.4	Preparation of samples	49
2.4.1	Preparation of powder	49
2.4.2	Preparation of green compact	50
2.4.3	Sintering	50
2.5	Density and porosity	54
2.6	Conclusions	59
Chapter 3	Metallurgical characterisation of non-functionally graded and functionally graded materials	60
3.1	Introduction	60
3.2	Microstructural analysis	60
3.2.1	Non-functionally graded material samples	60
3.2.2	Functionally graded material samples	66
3.3	X-ray diffraction (XRD)	69
3.3.1	Non-functionally graded materials	69
3.3.2	Functionally graded materials	71

3.4	Energy dispersive spectroscopy (EDS)	72
3.5	Conclusions	74
Chapter 4	Mechanical characterisation of non-FGMs/FGMs	76
4.1	Introduction	76
4.2	Tensile test	76
4.3	Fractography of tensile test samples	83
4.4	Comparison of experimental Young's modulus and Poisson's ratio with micromechanics prediction	85
4.5	Hardness of Al/Al ₂ O ₃ non-FGMs	95
4.6	Charpy impact energy of Al/Al ₂ O ₃ non-FGMs	96
4.7	Micro-hardness of Al/Al ₂ O ₃ and Al/B ₄ C FGMs	99
4.8	Conclusions	101
Chapter 5	Fracture characterisation of non-FGMs/FGMs	104
5.1	Introduction	104
5.2	Fracture toughness test	104
5.3	Fractography of fracture toughness test specimen	113
5.4	Conclusions	116
Chapter 6	Quasi static crack growth	117
6.1	Introduction	117
6.2	Quasi static crack growth measurement	117
6.3	Calculation of fracture toughness and CTOD	119
6.4	Crack on stiff side	121
6.5	Crack on compliance side	126
6.6	Fractography of quasi static crack growth test specimens	129
6.7	Conclusions	132

Chapter 7	Conclusions and Scope for future research work	133
7.1	Conclusions from present work	134
7.2	Scope for future work	136
References		137
List of publication from the thesis		152
Brief Bio data of the Author		154

List of Figures

Figure No.	Title	Page No.
1.1	Microstructure of typical FGM (Koizumi, 1993).	3
1.2	Potential fields of application of FGM.	4
1.3	FGM with crack initially oriented (a) perpendicular to gradation direction and (b) Parallel to gradation direction (Konda and Erdogan, 1994).	17
1.4	Crack tip interference for glass/epoxy (a, b) FGM (c) bi-material (d) homogeneous material (Rousseau and Tippur, 2000).	21
2.1	Palette of Al powder prepared for XRF testing.	40
2.2	Spectra of (a) aluminum and (b) alumina powders obtained from XRF tests.	42
2.3	XRD of aluminum (Al), boron carbide (B ₄ C) and alumina (Al ₂ O ₃) powders.	44
2.4	SEM of Al, Al ₂ O ₃ powders, 90Al/10Al ₂ O ₃ , 80Al/20Al ₂ O ₃ , 70Al/30Al ₂ O ₃ and B ₄ C of grade (SG 400, SG 600, SG 800, SG 1000 at magnifications of 500X, 1000X and 4000X.	47
2.5	Flow chart of FGM and non-FGM samples preparation.	49
2.6	Variation of Young's modulus and density with sintering temperature at constant pressure of 150 bar and 45 minutes duration.	52
2.7	Variation of Young's modulus and density with sintering pressure at constant temperature of 600 °C and 45 minutes duration.	52
2.8	Variation of Young's modulus and density with sintering duration at constant temperature of 600 °C and 300 bar pressure.	53

2.9	Aluminum specimen after sintering beyond optimum temperature of 600°C, pressure of 300 bar and time duration of 90 minutes.	53
2.10	Different stages of preparation of samples using powder metallurgy.	55
2.11	Variation of porosity with weight fraction of ceramics.	58
3.1	Optical microstructure at 100X of Al/Al ₂ O ₃ non-functionally graded material sample.	63
3.2	SEM microstructure of (i) 100Al, (ii) 90Al/10Al ₂ O ₃ , (iii) 80Al/20Al ₂ O ₃ , (iv) 70Al/30Al ₂ O ₃ , (v) 60Al/40Al ₂ O ₃ , (vi) 50Al/50Al ₂ O ₃ non-FGM samples at 100X, (vii) Bonding at agglomeration free zone, (viii) Bonding at agglomeration zone.	65
3.3	SEM microstructural image of (i) 95Al/5B ₄ C SG400, (ii) 90Al/10B ₄ C SG400, (iii) 85Al/15B ₄ C SG400 and (iv) 80Al/20B ₄ C SG400 samples.	66
3.4	(a) Optical microstructure of Al/Al ₂ O ₃ FGM sample and (b) Variation of designed and measured weight fractions of alumina with distance from 100% aluminum face.	67
3.5	SEM microstructural image of (i) 100Al-97.5Al/2.5Al ₂ O ₃ , (ii) 90Al/10Al ₂ O ₃ -87.5Al/12.5Al ₂ O ₃ , (iii) 80Al/20Al ₂ O ₃ -77.5Al/22.5Al ₂ O ₃ and (iv) 72.5Al/27.5Al ₂ O ₃ - 70Al/30Al ₂ O ₃ samples.	68
3.6	XRD of (a) Al powder, Al ₂ O ₃ powder, 90Al/10Al ₂ O ₃ , 80Al/20Al ₂ O ₃ , 70Al/30Al ₂ O ₃ , 60Al/40Al ₂ O ₃ and 50Al/50Al ₂ O ₃ composites and (b) Al powder, B ₄ C powder, 90Al/10B ₄ C, 80Al/20B ₄ C composites.	70
3.7	XRD of (a) Al powder, (b) Al ₂ O ₃ powder, (c) FGM sample at different distances from 100 aluminium end.	71
3.8	EDS pattern of Al/ Al ₂ O ₃ samples.	73
3.9	EDS pattern of Al/B ₄ C samples.	73
4.1	Dimensions of tensile test specimen.	80
4.2	Tensile test set up.	81

4.3	Stress- strain diagram of different Al/Al ₂ O ₃ composites.	81
4.4	Variation of 0.2% yield stress, UTS, Young's modulus and % elongation with weight fraction of alumina.	82
4.5	Representative SEM fractography of tensile test samples (a) 100Al at 300X, (b) 100Al at 3000X, (c) 90Al/10Al ₂ O ₃ at 300X, (d) 90Al/10Al ₂ O ₃ at 3000X, (e) 80Al/20Al ₂ O ₃ at 300X, (f) 80Al/20Al ₂ O ₃ at 3000X, (g) 60Al/40Al ₂ O ₃ at 300X, (h) 60Al/40Al ₂ O ₃ at 3000X.	84
4.6	Impulse excitation setup for measurement of elastic properties	87
4.7	Comparison of experimentally determined Young's modulus with micromechanics bounds for different Al ₂ O ₃ weight fractions for Al/Al ₂ O ₃ non-FGM samples.	88
4.8	Comparison of experimentally determined Young's modulus with micromechanics bounds for different weight fractions of Al/B ₄ C non-FGM samples.	91
4.9	Comparison of experimentally determined Young's modulus with micromechanics single value predictions (closer to the experimental value) for different ceramic weight fractions: (a) Al/Al ₂ O ₃ (b) Al/B ₄ C non-FGM samples.	92
4.10	Comparison of experimentally determined Poisson's ratio with micromechanics bounds for different ceramic weight fractions: (a) Al/Al ₂ O ₃ (b) Al/B ₄ C non-FGM samples.	94
4.11	Variation of Rockwell hardness of Al/Al ₂ O ₃ non-FGM samples with weight fraction of Al ₂ O ₃ .	95
4.12	Charpy energy set-up used for testing.	97
4.13	Variation of charpy impact energy of Al/Al ₂ O ₃ non-FGM samples with weight fraction of Al ₂ O ₃ .	98

4.14	Comparison of experimental microhardness with micromechanics bounds along the gradation direction: (a) Al/Al ₂ O ₃ (b) Al/B ₄ C FGM samples.	100
5.1	Specimen and Setup for measurement of fracture toughness.	105
5.2	Load versus crack mouth opening displacement (CMOD) for a) 100Al, (b) 90Al/10Al ₂ O ₃ , (c) 80Al/20Al ₂ O ₃ (d) 70Al/30Al ₂ O ₃ , (e) 60Al/40Al ₂ O ₃ , (f) 50Al/50Al ₂ O ₃ .	111
5.3	Comparison of experimentally determined K _{IC} with micromechanics bounds for different ceramic weight fractions for Al/Al ₂ O ₃ .	112
5.4	Comparison of experimentally determined K _{IC} for different particle size with micromechanics bounds for different ceramic weight fractions for Al/B ₄ C.	112
5.5	Representative SEM fractography of (a) 100Al at 500X, (b) 90Al/10Al ₂ O ₃ at 500X, (c) 90Al/10Al ₂ O ₃ at 500X, (d) 90Al/10Al ₂ O ₃ at 1000X, (e) 80Al/20Al ₂ O ₃ at 500 X, (f) 60Al/40Al ₂ O ₃ at 1000X for fracture toughness test.	114
5.6	Representative SEM fractography of fracture toughness test specimens: (a) 95Al/5B ₄ C SG400 at 500X (b) 90Al/10 B ₄ C SG400 at 500X (c) 85Al/15B ₄ C SG400 at 500X and (d) 85Al /15B ₄ C SG400 at 2000X.	115
6.1	Set-up for measurement of crack growth using crack gauge.	119
6.2	Definition of area (A _{pl}) for J _{pl} calculation.	120
6.3	Variation of load, crack length and load line displacement with time for crack on stiff side (FGM I).	124
6.4	Load versus load point displacement curve of FGM samples for crack on stiff side (FGM I).	124
6.5	Variation of weight fraction of alumina with crack tip location for FGM samples for crack on stiff side.	125

6.6	Variation of fracture toughness and CTOD with location of crack tip in FGM samples for crack on stiff side (FGM I).	125
6.7	Variation of load, crack length and load line displacement with time for crack on compliance side (FGM II).	128
6.8	Representative SEM fractography of FGM when crack on the stiff side (FGM I).	131
6.9	Fracture path of FGM samples for crack on stiff side (FGM I),	131
6.10	Representative SEM fractography of FGM when crack on the compliance side (FGM II).	131
6.11	Fracture path of FGM samples for crack on compliance side (FGM-II)	132

List of Tables

Table No.	Title	Page No
2.1	Composition of Al and Al ₂ O ₃ powder from XRF data	41
2.2	Crystalline domain size (μm) evaluated using different methods from XRD data of aluminum, alumina and boron carbide powders	44
2.3	Dimensions and quantities of various non-FGMs and FGMs samples used during characterizations.	56
2.4	Density in kg/m ³ and porosity of Al/Al ₂ O ₃ and Al/B ₄ C samples for different ceramic weight fraction.	56
2.5	Comparison of porosity of Al/Al ₂ O ₃	59
3.1	Measured particle size of alumina from different non-FGM samples	61
4.1	Contribution of strengthening mechanisms to 0.2% yield stress for Al/Al ₂ O ₃ composite	79
4.2	Parameters used to determine predicted strength enhancement for Al/Al ₂ O ₃ composite	79
4.3	Comparison of 0.2% proof stress, UTS and % elongation of Al/Al ₂ O ₃	82
4.4	Comparison of experimentally measured Young's modulus and micromechanics single value predictions	88
4.5	Comparison of Young's modulus of Al/Al ₂ O ₃	93

4.6	Comparison of experimentally measured Poisson's ratio with micromechanics bounds	94
4.7	Comparison of Rockwell hardness (RB) of Al/Al ₂ O ₃	96
4.8	Comparison of microhardness (HV) of Al/Al ₂ O ₃	101
5.1	Fracture toughness of Al/Al ₂ O ₃ and Al/B ₄ C composites for different particle size with weight fraction of ceramic	107
6.1	Specifications of crack gauge	118

Nomenclature

Roman Symbols

A	:	Constant parameter (IET)
A_{pl}	:	Plastic part of area under load displacement curve
a	:	Crack length
a_o	:	Initial crack length
a_p	:	Physical crack length
$\frac{a}{W}$:	Crack length to width ratio
u_i ($i = x, y$)	:	Displacement in x and y directions
B	:	Thickness of specimen
b	:	Magnitude of Burgers vector
b_o	:	Ligament length
\tilde{C}	:	Constant parameter (IET)
C	:	Ravichandran's constant
c	:	Ravichandran's modified constant
d	:	Crystalline size
d_2	:	Particle diameter
E	:	Young's modulus
E_{30Al}	:	Young's modulus of 70Al/30Al ₂ O ₃ composite
E_{100Al}	:	Young's modulus of 100% aluminum

E_i ($i = 1, 2$)	: Young's modulus of phase 1 and 2/instantaneous value of Young's modulus at crack tip
E_0	: Young's modulus at original crack tip
$E(x)$: Variation of Young's modulus with x coordinate
E^l	: Lower bound of Young's modulus
E^u	: Upper bound of Young's modulus
f_r/f_t	: Flexural/torsional resonant frequency
G	: Shear modulus (Modulus of rigidity)
\tilde{G}	: Energy release rate
G_i ($i = 1, 2$)	: Shear modulus of phase 1 and 2
$G(x)$: Variation of shear modulus with space
G^l	: Lower bound of shear modulus
G^u	: Upper bound of shear modulus
$g_i^I(\theta)(i = x, y)$: Mode-I angular distribution functions at crack tip
$g_i^{II}(\theta)(i = x, y)$: Mode-II angular distribution functions at crack tip
J	: J -integral
J_e/J_{pl}	: Elastic and plastic parts of J Integral
K	: Bulk modulus
K_Q	: Provisional Stress intensity factor
K_I, K_{II}, K_{III}	: Stress intensity factor in Mode-I, Mode-II and Mode-III
K_i ($i = 1, 2$)	: Bulk Modulus of phase 1 and 2
$K_1(V_2)/K_2(V_2)$: Effective bulk modulus predicted by Kerner method

K_{IC}	:	Fracture toughness
$(K_{IC})_1$:	Fracture toughness of phase 1
$(K_{IC})_2$:	Fracture toughness of phase 2
$K_{IC}(x)$:	Variation of fracture toughness with x coordinate
L	:	Length
m	:	Mass
m_a, m_w	:	Mass of specimen in air and water
P	:	Load
\tilde{P}	:	Porosity
P_{max}	:	Maximum load value
$P(V_2)$:	Interpolation function
q	:	Stress to strain transfer coefficient
r	:	Radius of particle
\tilde{r}	:	Radial distance from crack tip
T	:	Temperature
\tilde{T}	:	T-stress
t	:	Time
S	:	Span/Distance between two roller supports
u_i ($i = x, y$)	:	Displacement in x and y directions
V	:	Volume fraction
V_i ($i = 1, 2$)	:	Volume fraction of phase 1 (matrix) and phase 2 (reinforcement)

W	:	Width
\hat{W}	:	Strain energy density
$w_i (i = 1, 2)$:	Weight fraction of phase 1 and phase 2
x	:	Longitudinal coordinate
y	:	Transverse coordinate

Greek Notations

α	:	Kink angle
α_m / α_p	:	Coefficient of thermal expansion of matrix and particle
$\Delta\alpha$:	Difference of coefficient of thermal expansion between two phases
β	:	Full width at half maximum
$\tilde{\beta}$:	Dislocation strengthening coefficient
δ	:	Crack tip opening displacement (CTOD)
$\tilde{\delta}$:	Interparticle spacing
ε	:	Strain
$\varepsilon_1, \varepsilon_2$:	Principal strains
η_{pl}	:	Constant for J integral
λ	:	Wavelength of the incident X-ray
$\hat{\lambda}$:	Microvoid spacing
θ	:	Diffraction angle corresponding to a peak
$\tilde{\theta}$:	Location of a point w.r.t. crack axis

ρ	:	Density
ρ_s	:	Density of sintered specimen
ρ_t	:	Theoretical density
ρ_w	:	Density of water
ρ_1, ρ_2	:	Density of phase 1 and phase 2
σ_1, σ_2	:	Principal stresses
$\sigma_{.2}$:	0.2% proof stress
σ_y	:	Yield stress
σ_u	:	Ultimate tensile strength
σ_{ij}	:	Stress tensor
$\Delta\sigma$:	Gain in yield strength
$\Delta\sigma_{load}$:	Yield strength enhancement due to bearing forces
$\Delta\sigma_{Hall-Petch}$:	Change in yield strength due to change in grain size of the matrix
$\Delta\sigma_{Orowan}$:	Orowan strengthening
$\Delta\sigma_{CTE}$:	Strengthening due to change in temperature
ν	:	Poisson's ratio
ω_0	:	Constant used in crack tip displacement field

Abbreviations

ASTM	:	American society for testing and materials
BEM	:	Boundary element method
CEQ	:	Charpy energy equivalent
CGS	:	Coherent gradient sensing
CIT	:	Cold isostatic pressing
CMC	:	Ceramic matrix composite
CMOD	:	Crack mouth opening displacement
COD	:	Crack opening displacement
CPA	:	Coherent potential approximation
CTOD	:	Crack tip opening displacement
CVD	:	Chemical vapour deposition
DCB	:	Double cantilever beam
DIC	:	Digital image correlation
ECO	:	Ethylene carbon monoxide
EDS	:	Energy dispersive spectroscopy
EMA	:	Effective medium approximation
ERR	:	Energy release rate
FEM/FEA	:	Finite element method/analysis
FWHM	:	Full width at half maximum
FESEM	:	Field emission scanning electron microscopy

FGM	:	Functionally graded material
FLM	:	Fuzzy logic method
HCM	:	Hopkins-Chamis method
HEQ	:	Hardness equivalent
HIT	:	Hot isostatic pressing
HSLB/HSUB	:	Hashin - Shtrikman lower/upper bounds
HTM	:	Halpin–Tsai method
IET	:	Impulse excitation technique
IKM	:	Inverse Kerner method
IMTM	:	Inverse Mori-Tanaka method
IPC	:	Interpenetrating phase composite
IWTM	:	Inverse Wakashima and Tsukamoto method
JCPDS	:	Joint committee on powder diffraction standards
KM	:	Kerner method
MMC	:	Metal matrix composite
MRLB/MURB	:	Modified Ravichandran lower/upper bounds
MROM	:	Modified rule of mixture
MTM	:	Mori-Tanaka method
NDT	:	Non-destructive test
Non-FGM	:	Non functionally graded material
OP	:	Optical microscopy
PM	:	Powder metallurgy

PMC	:	Polymer matrix composite
PSZ	:	Partially stabilised Zirconia
PVD	:	Physical vapour deposition
RLB/RUB	:	Ravichandran lower/upper bounds
ROM/ RROM	:	Rule of mixture/reciprocal rule of mixture
SCM	:	Self consistent method
SEM	:	Scanning electron microscopy
SENB	:	Single edge notched beam
SFF	:	Solid free form
SG	:	Specific grid
SIF	:	Stress intensity factor
TPB	:	Three point bending
TTOM	:	Tamura-Tomoto-Ozara model
UTS	:	Ultimate tensile strength
UV	:	Ultraviolet
VDT	:	Vapour deposition technique
WTM	:	Wakashima and Tsukamoto method
XRD	:	X-ray diffraction
XRF	:	X-ray fluorescence
YS	:	Yield strength
ZLB/ZUB	:	Zimmerman lower/upper bounds